# Water oxidation catalysed by a mononuclear $Co^{II}$ polypyridine complex; possible reaction intermediates and the role of the chloride ligand

Biswanath Das, Andreas Orthaber, Sascha Ott*, and Anders Thapper*

Department of Chemistry, Ångström Laboratory, Uppsala Universitet, Box 523, 75120 Uppsala, Sweden

**A. Experimental Section:**

**Instrumentation:**

**$^1$H NMR** spectra were run on a JEOL-400 MHz spectrometer at 293K. Chemical shifts are given in ppm and referenced internally to the residual solvent signal. **ESI-MS** was performed on a Finnigan LCQ Deca XP MAX. The **UV-Vis** absorption spectra were measured on a Varian Cary 50 instrument.

**Cyclic voltammetry** and differential pulse voltammetry were carried out using an Autolab potentiostat with a GPES electrochemical interface (Eco Chemie). Cyclic voltammograms were recorded at a scan rate of 50 mV $s^{-1}$ (unless specified). The working electrode was a glassy carbon disc (diameter 3 mm). The surface of the electrode was routinely polished with an alumina(0.05 mm)-water slurry on a felt surface, immediately prior to use. A glassy carbon rod was used as counter electrode. In case of aqueous medium Ag/AgCl (with saturated KCl aqueous solution) reference electrode was used and $Ag/AgNO_3$ reference electrode was used in acetonitrile solution.

**Oxygen evolution** was monitored using a standard Clark-type oxygraph electrode (Hansatech Instruments), separated from the sample solution by a Teflon membrane. The signal was recorded for the entire duration of the experiment at 0.1 sec intervals using the Oxygraph+ software (Hansatech Instruments). The maximum turnover frequency (TOFmax) was determined at the steepest slope of the oxygen evolution curve. The signal was calibrated using air saturated aqueous solutions ($[O_2]$ = 282 µM, T = 20.1 °C).[1]

**Elemental analyses** were performed by Analytische Laboratorien GmbH, Lindlar, Germany.

**Dynamic light scattering** experiments were performed using uniphase He-Ne laser emitting vertically polarized light at a wavelength of ~465 nm (power 22 mW) and two avalanche photo diodes (PerkinElmer, Canada) working in cross auto correlation mode. Data was collected at 294±0.5 K. The scattering angle was set to 90° from the incident laser. The intensity correlation curves were analyzed with the ALV-500/E/EPP + ALV-60XO-win V3.0.2.3 software based on standard CONTIN analysis.

**EPR measurements** were performed using a Bruker ESR-500 spectrometer, equipped with an ER 4122SHQ resonator equipped with an ESR900 cryostat and an Oxford ITC503 temperature controller.

**X-ray diffraction**: All the measurements were performed using graphite-monochromatized Mo $K_\alpha$ radiation at 100K using a Bruker D8 APEX-II equipped with a CCD camera. The structure was solved by direct methods (SHELXS-2014) and refined by full-matrix least-squares techniques against $F^2$ (SHELXL-2014).[2] The non-hydrogen atoms were refined with anisotropic displacement parameters. The H atoms of the methyl groups were refined with common isotropic displacement parameters for the H atoms of the same group and idealized geometry and C-H distances of 0.98 Å. Aromatic H atoms are place at idealized positions at a distance of 0.95 Å.

The structure of **2** was optimized with a disordered toluene molecule around a special position (isotropically refined, before squeeze). Due to substantial residual electron density and due to the unresolved disorder the squeeze algorithm was applied. After removing the toluene entity the excess electron density in the accessible voids was squeezed and the model was further refined to the new data.[3]

**Syntheses:** Chemicals were purchased from Aldrich Chemicals and used without further purification unless noted otherwise. The ligand $(Py)_5(OH)_2$ (**1**) was prepared following the procedure reported by Stack et.al.[4] The penta-pyridylcarbinol ligand (**1**) was recrystallized from acetone (with 52% overall yield). Shining white crystals of **1** was obtained by slow evaporation of acetone from the concentrated solution inside 4 degree Celsius fridge.

$^1$H NMR (400 MHz, $CDCl_3$): 7.13 (4 H, t of d), 7.43 (1 H, m), 7.45 (2 H, m), 7.50 (4 H, m), 7.72 (4 H, m), 8.47 (4 H, m). ESI-MS: calculated for $(1+H^+)$ $[(Py)_5(OH)_2(H)]^+$ m/Z: 448.17; found: 448.12;

$[Ru^{III}(bpy)_3](ClO_4)_3$ was prepared according to literature,[5] $[Ru^{II}(bpy)_3](ClO_4)_2$ was prepared by anion exchange form $[Ru^{II}(bpy)_3]Cl_2$ (Aldrich) and recrystallized from EtOH.

**Preparation of 2**. $[Co^{II}(Py)_5(OH)_2(Cl)](BF_4)$ was prepared by adding 5ml methanol solution of $Co(BF_4)_2.6H_2O$ (0.15 g, 0.45mmol) to a 20ml stirring methanol solution of **1** (0.2 g, 0.45mmol), followed by addition of 0.03 g (0.51 mmol) of NaCl and continuous stirring . The brown precipitate of **2** formed over a period of 1 h of stirring, was isolated from the methanol solution by filtration and was washed with 5 ml ice cold methanol-$H_2O$ (5:1) twice to remove all the salt impurities, followed by drying overnight under vacuum gives 0.21 g of brown powder of **2** with 74% yield. Dissolving the brown precipitate in 10:1 Acetonitrile-Toluene solvent and slow evaporation of the solvent over a period of seven days leads to shining black brown crystal of X-ray diffraction quality of **2** (Fig S1).

Elemental analysis calculated (%) for $[Co^{II}(Py)_5(OH)_2(Cl)](BF_4).3H_2O$: C, 47.5; H, 3.99; N, 10.26. Found: C, 48.35; H, 3.86; N, 8.78. ESI-MS: calculated for $[Co^{II}(Py)_5(OH)_2(Cl)]^+$ m/Z: 541.07; found: 541.10; for $[Co^{II}(Py)5(OH)(O)]^+$ m/Z: 505.09; found 505.10 and for $[Co^{II}(Py)_5(OH)_2]^{2+}$ m/Z: 253.05; found 253.10. UV-Vis ($CH_3CN$): λmax 588 nm (ε= 860 $M^{-1}$ $cm^{-1}$), 685 nm (ε= 1180 $M^{-1}$ $cm^{-1}$) and a broad peak at 660 nm (ε= 1020 $M^{-1}$ $cm^{-1}$). Cyclic voltametric experiment in MeCN shows an irreversible wave at -0.21V [Co(I)/Co(II)] and two quasi reversible redox waves at +0.65V [Co(II)/Co(III)] and +1.05V [Co(III)/Co(IV)] vs NHE.

**Table S1.** Crystal data and structure refinement for 2

| Crystal data | Before Squeeze | After Squeeze |
|---|---|---|
| CCDC-No. | 1050730 | |
| Empirical formula | $C_{27}H_{21}ClCoN_5O_2$, $BF_4$, $C_7H_8$ | $C_{27}H_{21}ClCoN_5O_2$ |
| Formula weight | 723.85 | 527.86 |
| Crystal description | Brownish-black plate | |
| Crystal size | 0.25 x 0.20 x 0.10 | |
| Crystal system, space group | Orthorhombic, P b c m | |
| Unit cell dimensions: a | 8.6043(10) | |
| b | 16.622(2) | |
| c | 21.331(3) | |
| Volume | 3050.8(6) | |
| Z | 4 | |
| Calculated density | 1.576 Mg/m³ | 1.149 |
| F(000) | 1492 | 1084 |
| Linear absorption coefficient μ | 0.717 $mm^{-1}$ | 0.676 |
| Absorption correction | multi-scan, SADABS 2008 | |
| Max. and min. transmission | 0.6349 and 0.7454 | |
| Unit cell determination | $1.9 < \Theta < 27.0°$ | |
| | 2586 reflections used at 100K | |
| | | |
| Data collection | | |
| Temperature | 100(2)K | |
| Diffractometer | Bruker APEX-II CCD | |
| Radiation source | fine-focus sealed tube | |
| Radiation and wavelength | $MoK_\alpha$, 0.71073Å | |
| Monochromator | Graphite | |
| Scan type | ω scans | |
| Θ range for data collection | $1.9 < \Theta < 27.0°$ | |
| Index ranges | $-10 \le h \le 10$, $-12 \le k \le 10$, $-26 \le l \le 23$ | |
| Reflections collected / unique | 12839/ 3322 | |
| Significant unique reflections | 2594 with $I > 2\sigma(I)$ | |
| R(int), R(sigma) | 0.0422, 0.0454 | |
| Completeness to $\Theta_{max}$ | 98.8% | |
| | | |
| Refinement | | |
| Refinement method | Full-matrix least-squares on $F^2$ | |
| Data / parameters / restraints | 3322/ 213/ 0 | 3322/ 183/ 0 |
| Goodness-of-fit on $F^2$ | 1.038 | 0.562 |
| Final R indices [$I > 2\sigma(I)$] | R1 = 0.0888, wR2 = 0.2464 | R1 = 0.0428, wR2 = 0.1251 |
| R indices (all data) | R1 =0.1105, wR2 = 0.2683 | R1 = 0.0588, wR2 = 0.1485 |
| Weighting scheme | $w=1/[\sigma^2(F_o^2)+(aP)^2+bP]$ where $P=(F_o^2+2F_c^2)/3$ | |
| Weighting scheme parameters a, b | 0.1480, 20.6601 | 0.1475, 20.8833 |
| Largest $\Delta/\sigma$ in last cycle | 0.000 | 0.002 |
| Largest difference peak and hole | 1.971 and -1.142 e/Å³ | 0.496 and -0.628 e/Å³ |
| Structure Solution Program | SHELXS-2014 (Sheldrick, 2008) | |
| Structure Refinement Program | SHELXL-2014 (Sheldrick, 2008) | |

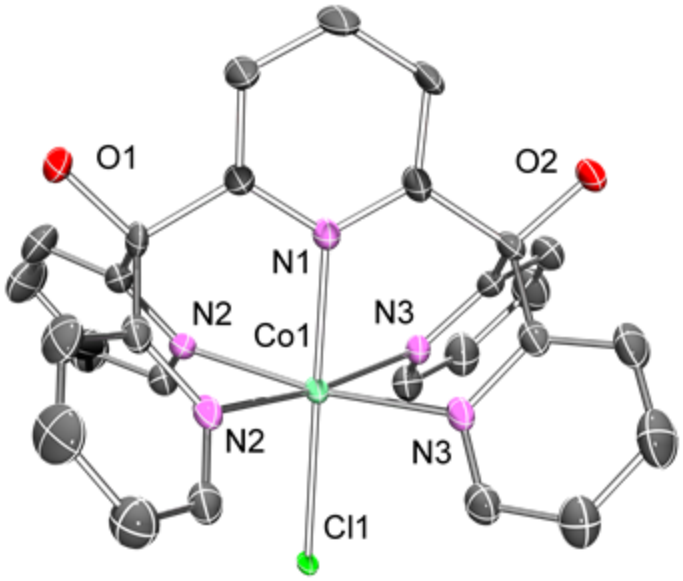


**Fig S1.** Crystal structure of **2** [$Co^{II}$(Py5OH)(Cl)]($BF_4$) (ellipsoids at 50% probability level). Hydrogen atoms and the counter anion were removed for clarity.

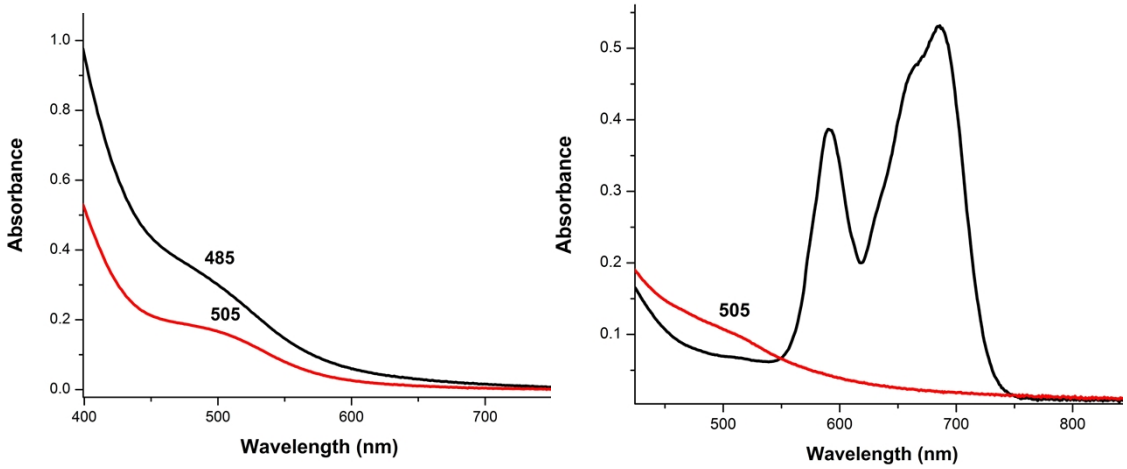


**Fig S2.** UV-Vis spectra of (a) **2** (0.5mM) (black) in water (borate buffer;pH8) and of the filtrate after reacting same solution of **2** with 2 eq of $AgBF_4$ in water(borate buffer;pH8) (red); (b) **2** (0.5mM) (black) in acetonitrile and of the filtrate after reacting same solution of **2** with 2 eq of $AgBF_4$ in water (red).

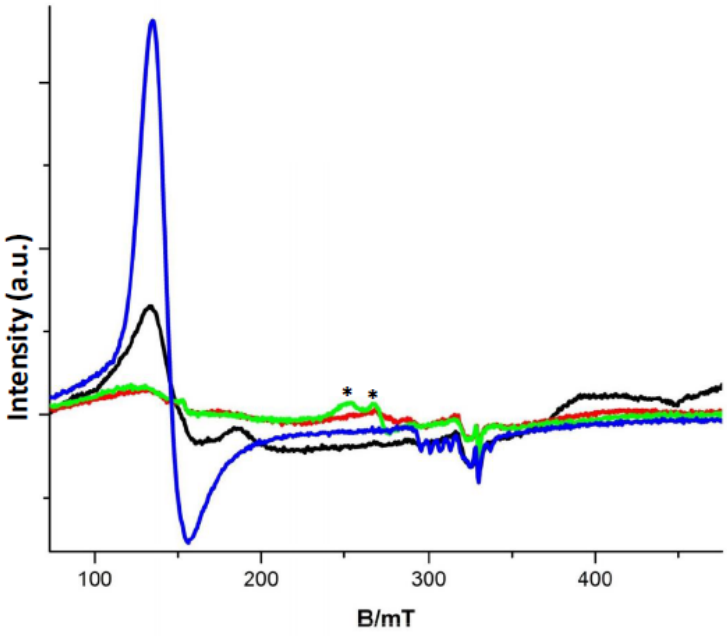


**Fig S3.** EPR spectra of **2** (0.5 mM) in borate buffer (0.2 M, pH 8) before (blue) and after addition of 1 (black), 2 (red), or 5 (green) $[Ru^{III}(bpy)_3](ClO_4)_3$. In the experiment ~2 eq of $[Ru^{III}(bpy)_3](ClO_4)_3$ is needed to oxidize **2** completely and after that development of characteristic $Ru^{III}$ EPR spectrum (*) was observed.[6] Temperature: 7 K, Microwave power: 20 μW, Modulation amplitude: 10 G.

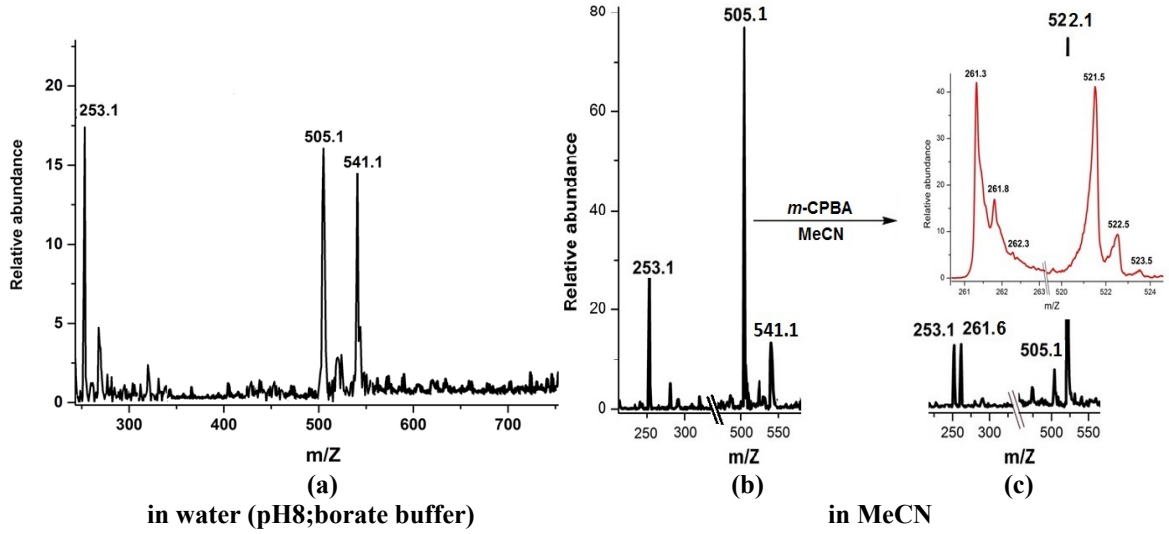


**Fig S4.** ESI-MS spectra of **2** in water (a), in MeCN (b) and after addition of 10eq of *m*-CPBA (c) at rapid positive detection mode. The inset of (c) is a magnification showing the characteristic isotope pattern of $\mathbf{2}^{ox}$.

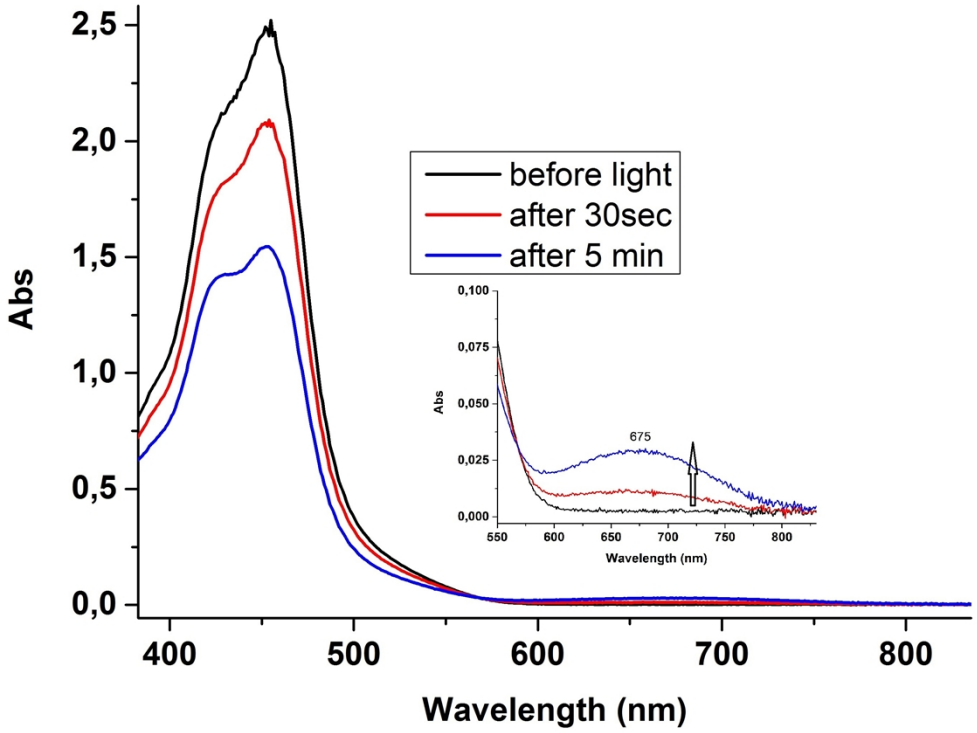


**Fig S5.** Spectral changes observed on illuminating (with 465 nm LED lamp) a solution of 2 (5.0 μM), $[Ru^{II}(bpy)_3](ClO_4)_2$ (0.15mM), $Na_2S_2O_8$ (3mM) in 0.2M borate buffer (pH 8)**.**

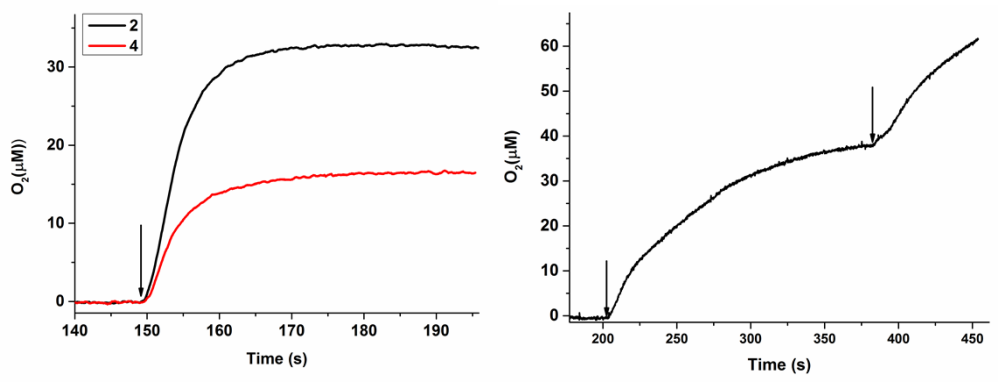


**a** **b**

**Fig S6.** (a) $[Ru^{III}(bpy)_3]^{3+}$ (200 μM) induced oxygen evolution experiments using **2** (2 μM, black) or *in situ* generated **4** (2 μM, red) as catalysts in pH 8 borate buffer (0.2 M). TON of ~15 was observed when the $Ru^{III}$:**2** was 100:1. TON of ~6.5 was observed when the $Ru^{III}$ : **4** was 100:1. No appreciable improvement of TON was observed increasing the $Ru^{III}$:**4** to 150:1. (b) Oxygen evolution experiment using **2** (2 μM) as catalyst in pH 8 borate buffer (0.2 M) and making two consecutive additions of $[Ru^{III}(bpy)_3]^{3+}$ (200 μM) demonstrating that the catalyst is active at the end of the first oxygen evolution. The arrows indicate when 100 μL of an aqueous $Ru^{III}$ solution (degased by Argon over a period of 30 Sec) was injected.

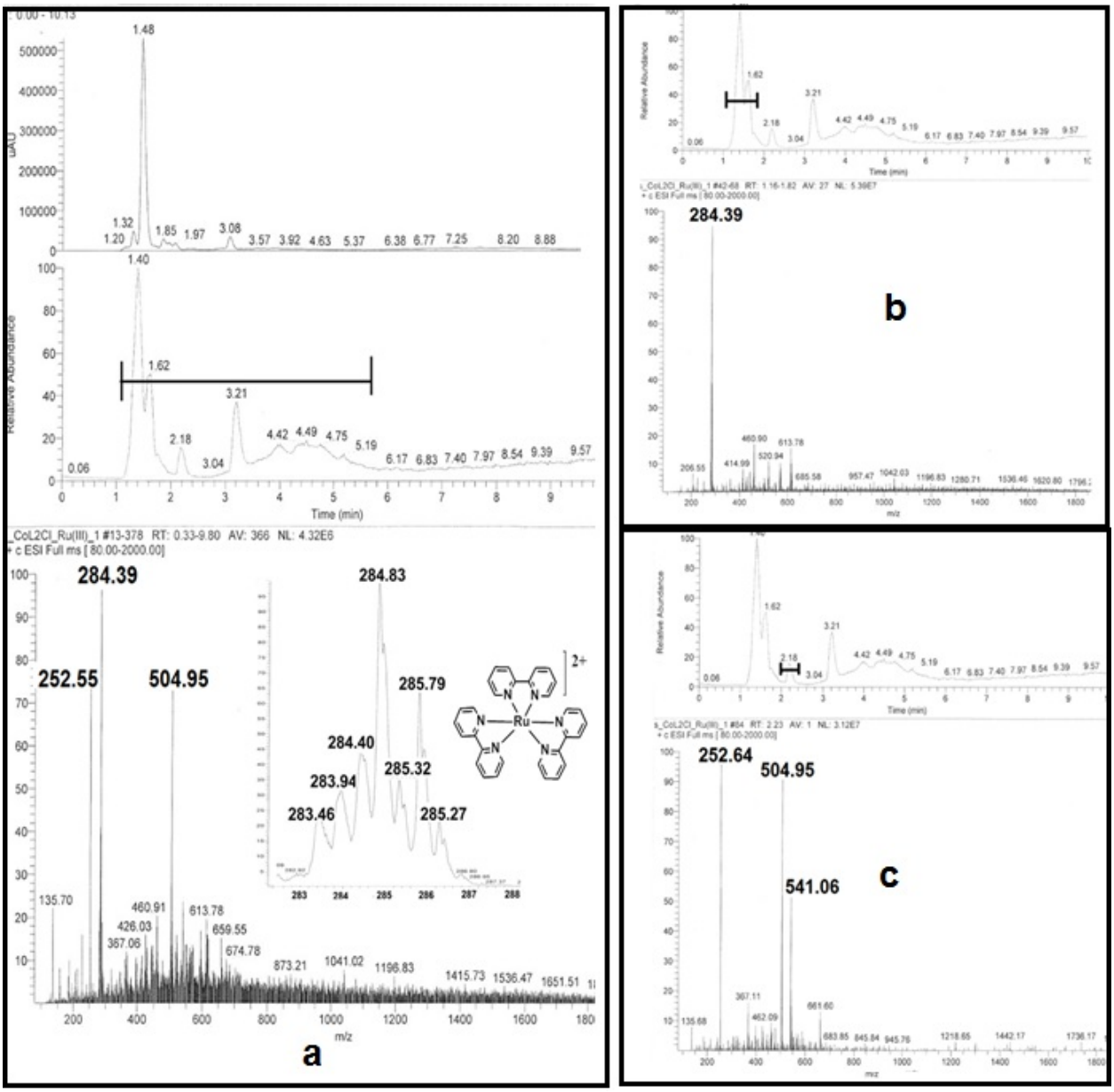


**Fig S7.** LC-ESI-MS spectra of the solution after Ru(III) induced water oxidation experiment using a Ru(III):**2** ratio 20:1. a) Mass spectrum of entire reaction mixture. Inset shows characteristic isotope pattern of $Ru(bpy)_3^{2+}$ species. b) Mass spectrum of the fraction with RT 1.4-1.8 (mostly $Ru(bpy)_3^{2+}$). c) Mass spectrum of the fraction with RT ~2.2 (mostly **2**).

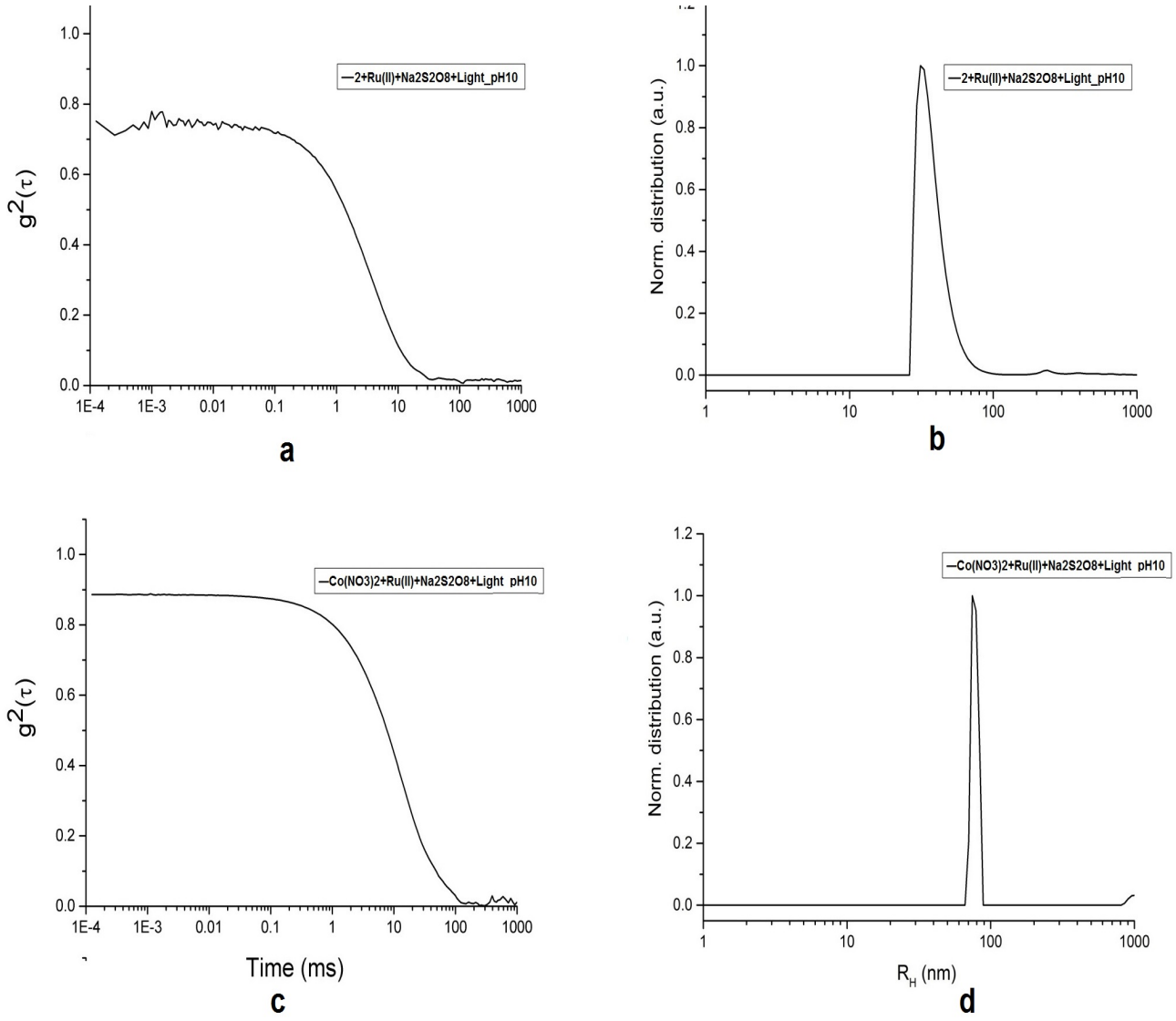


**Fig S8.** In a series of dynamic light scattering (DLS) experiments no trace of nanoparticle (within 1-1000 nm) formation was detected at pH8, pH9 (light induced water oxidation in borate buffer). At pH 10 (borate buffer), a trace corresponding to nanoparticle formation (hydrodynamic radius ~90 nm) was observed after illuminating the solution (**2**+$Ru^{(II)}$+ $S_2O_8^{2-}$+buffer) with 465nm light for 1 min. All the stock solutions were filtered using 0.45µm filter before mixing and no further filtration were performed afterwards. a) Correlation diagram b) Number distribution diagram of the solution (**2**+$Ru^{(II)}$+ $S_2O_8^{2-}$ at pH10 same condition as was used to detect oxygen evolution) after 1 min illumination. As a control we also studied nanoparticle formation using $Co(NO_3)_2$ salt under very similar experimental conditions. c) Correlation diagram d) Number distribution diagram of the solution ($Co(NO_3)_2$+$Ru^{(II)}$+ $S_2O_8^{2-}$ at pH10).

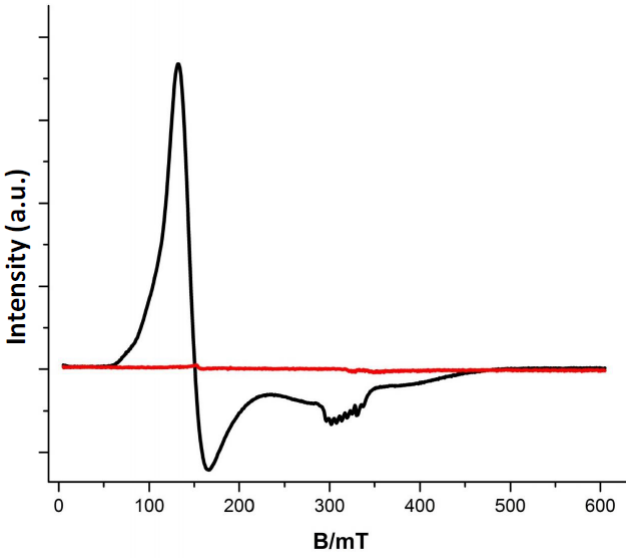


**Fig S9.** EPR spectra of **2** (0.5 mM) in MeCN before (black) and after (red) addition of 10eq *m*-CPBA (**2$^{ox}$**). The axial EPR signal is very similar to that observed in borate buffer with *g*-values of 4.5 and 2.1. Temperature: 7 K, Microwave power: 20 µW, Modulation amplitude: 10 G.

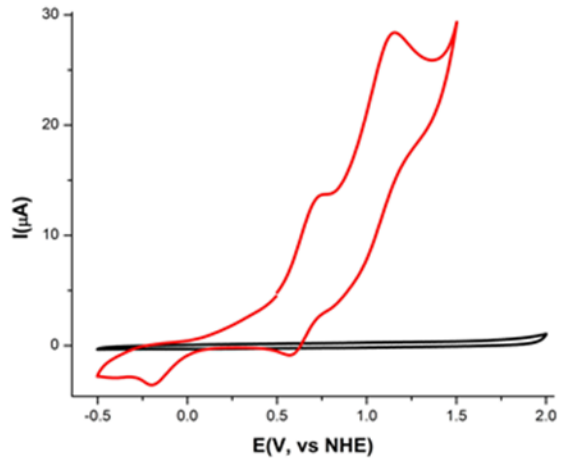


**Fig S10.** Cyclic voltammogram of **2** (5 mM) in MeCN (red). Scan rate = 50 mV/s; working electrode: Glassy carbon disc, counter electrode: Glassy carbon rod, reference electrode: $Ag/AgNO_3$ (10 mM), Supporting electrolyte: tetrabutyl ammonium perchlorate (0.1M). A background CV for neat MeCN with tetrabutyl ammonium perchlorate is shown in black.

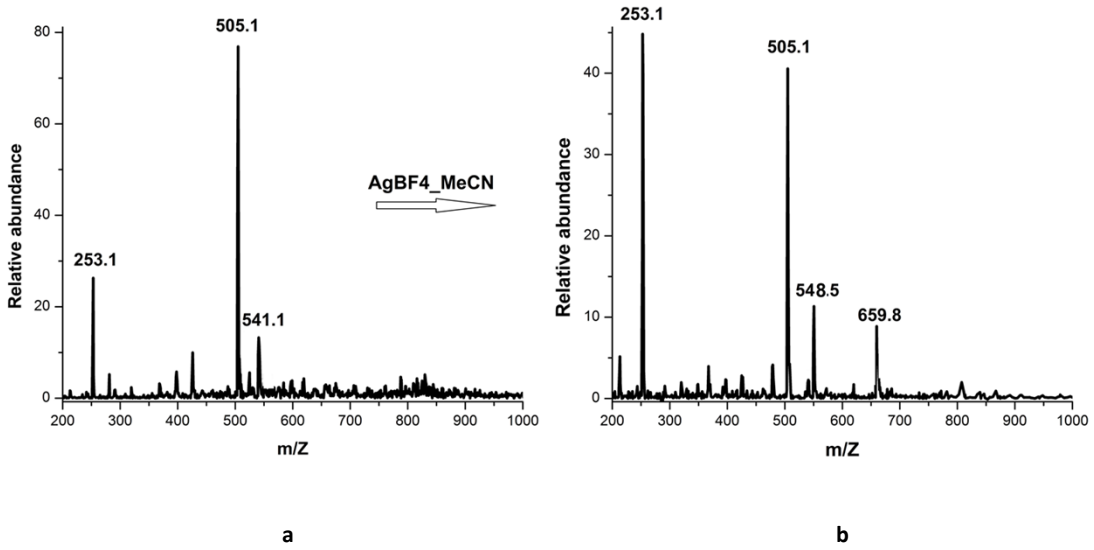


**Fig S11.** ESI-MS spectra of (a) **2** in MeCN (b) **3** in MeCN in positive detection mode.

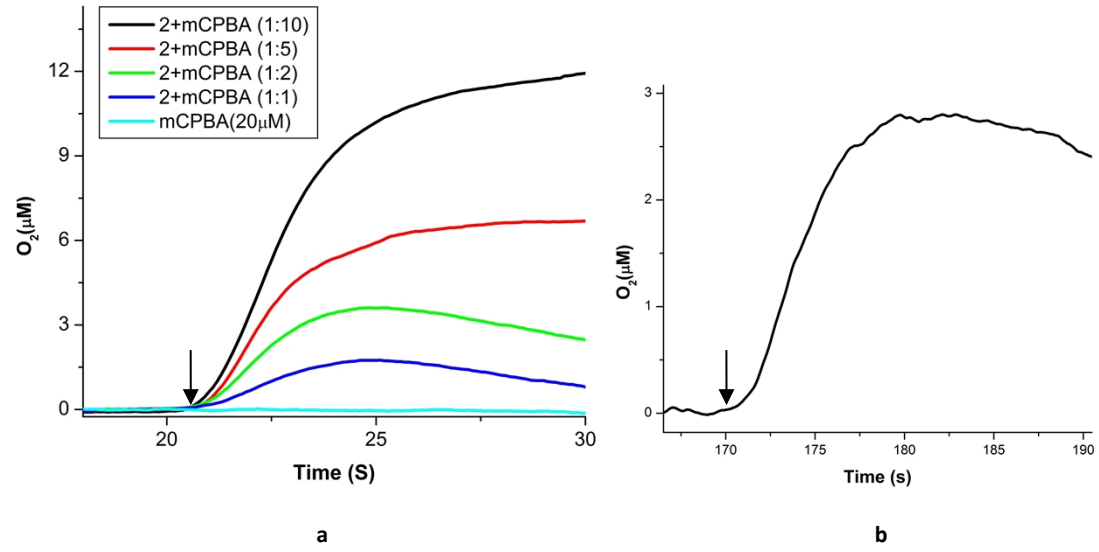


**Fig S12.** *m*-CPBA induced oxygen evolution experiment (a) using **2** as catalyst in acetonitrile + water (49:1) solution. Quantitative oxygen evolution was observed when less than 10 eq *m*-CPBA was used. Adding 20 eq *m*-CPBA did not give higher oxygen evolution and in a parallel UV-Vis experiment with 20 eq *m*-CPBA no regeneration of the characteristic spectrum of **2** (see Fig 4) was observed. No trace of oxygen evolution was detected when **2** was not added and (b) using in situ generated **3** as catalyst in acetonitrile + water (49:1) solution. TON of ~1.5 was observed when the **3** : *m*-CPBA was 1:10. Increasing the m-CPBA concentration to 1:20 (3: *m*-CPBA) did not improve TON to any appreciable value. Arrows indicate the time when degased (by Argon over a period of 30 Sec) 100 μL of m-CPBA was injected.

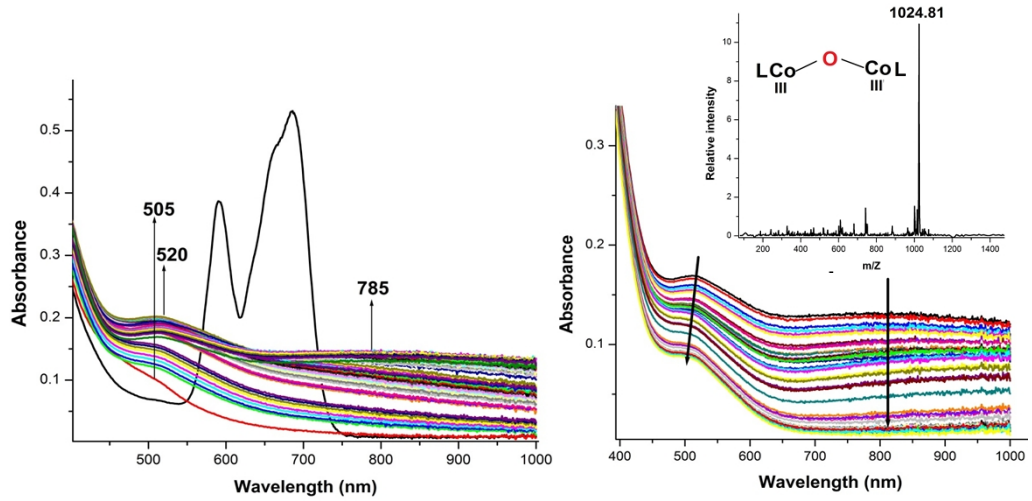


**Fig S13.** UV-Vis spectra of (a) **2** (0.5mM) (black line, strong absorption at 588 nm and 685 nm) in acetonitrile and of the filtrate after the reaction of the same solution of **2** (0.5mM) with 2 eq of $AgBF_4$ in MeCN (red line; absorption maxima at 505 nm). Generation of new species **($3^{ox}$)** was observed with absorption maximas at 520 and 785 nm (broad) on addition of 10 eq of *m*-CPBA over a period of 20 min. (b) UV-Vis spectral changes observed for **$3^{ox}$** over a period of 30 min. At least one additional species, with a $\lambda_{max}$ > 900 nm forms during the process. Inset shows the mass spectra **$3^{ox}$** and downward arrows indicate the decomposition of **$3^{ox}$** to **3** over a period of 30 min.

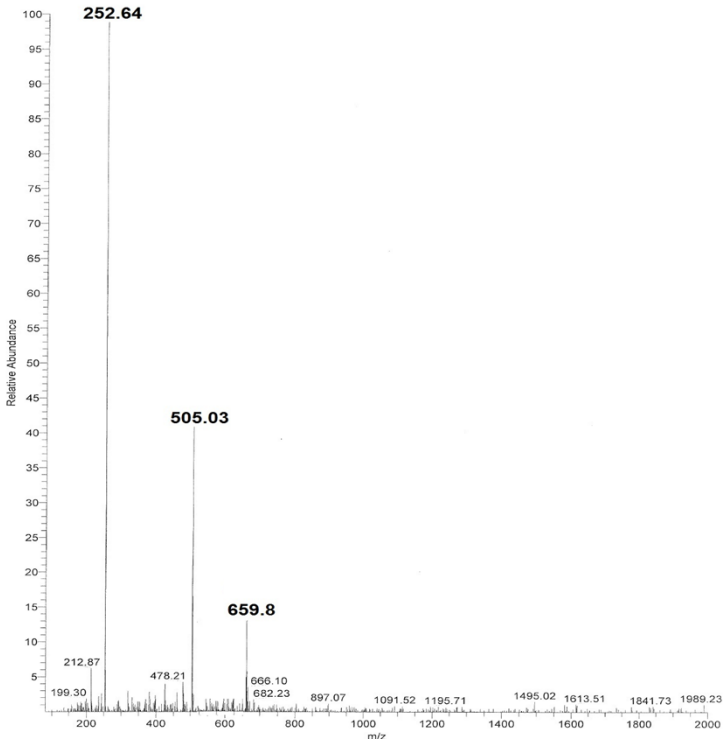


**Fig S14.** ESI-MS spectra of **4** in water in positive detection mode.

**B. References**


1. G. A. Truesdale and A. L. Downing, *Nature*, 1954, **173**, 1236-1236.

2. G. Sheldrick, *Acta Crystallogr., Sect. A: Found. Crystallogr.* 2008, **A64**, 112-122.
3. A. Spek, *J. Appl. Crystallogr.* 2003, **36**, 7-13.

4. R.T. Jonas, T. D**.** P. Stack, *J. Am. Chem. Soc.,* 1997, **119**, 8566-8567.

5. V. Y. Shafirovich, N. K. Khannanov and A. E. Shilov, *J. Inorg. Biochem.*, 1981, **15**, 113-129.

6. H. Agarwala, F. Ehret, A.D. Chowdhury, S. Maji, S. M. Mobin, W. Kaim and G. K. Lahiri, *Dalton Trans*., 2013, **42**, 3721.